Sand filtration in a water treatment plant: biological parameters responsible for clogging

L. Mauclaire, A. Schürmann, M. Thullner, S. Gammeter and J. Zeyer

ABSTRACT

Slow sand filtration is an established technique for the treatment of drinking water. However, clogging of these filters requires extensive maintenance. The clogging and hydraulic characteristics of slow sand filters operated under high flow rates were investigated in a drinking water plant that processes pre-treated lake water. Reasons for the clogging were evaluated by measuring physical, chemical and biological parameters of the interstitial water and the filter matrix. The biomass in the filters was characterised by quantifying bacterial abundance and activity as well as the concentration of extracellular polymeric substances (EPS). The results of this study showed that the clogging effects were to a large extent attributed to the presence of EPS. This microbial biomass reduced the pore space in the highly clogged parts of the filters by at least 7%, whereas the reduction due to particle deposition was not larger than 7%. Although the most severe clogging occurred in the top 5–10 cm of the filters where bacterial abundance and activity were highest, deeper layers of the filters were clogged, too.

Key words | bioclogging, extracellular polymeric substances (EPS), hydraulic conductivity, pore space, sand filtration, water treatment

L. Mauclaire[1]
A. Schürmann[2] (corresponding author)
M. Thullner[3]
J. Zeyer
Soil Biology,
Institute of Terrestrial Ecology,
Swiss Federal Institute of Technology (ETH),
Grabenstrasse 3, CH-8952 Schlieren,
Switzerland
E-mail: *Andreas.Schuermann@klzh.ch*
[1]Present address:
Geological Institute,
Swiss Federal Institute of Technology (ETH),
Sonneggstrasse 5, CH-8092 Zurich,
Switzerland
[2]Present address:
Official Food Control Authority of the Canton of Zurich,
Fehrenstrasse 15,
PO Box, CH-8030 Zurich,
Switzerland
[3]Present address:
Department of Earth Science-Geochemistry,
Utrecht University,
P.O. Box 80021,
NL-3508 TA Utrecht,
The Netherlands

S. Gammeter
Zurich Water Supply,
Hardhof 9, PO Box,
CH-8023 Zurich,
Switzerland

INTRODUCTION

Sand filtration is one of the oldest technologies for treating water in drinking water plants (Weber-Shirk & Dick 1997*a*). The simplicity of slow sand filtration makes the process attractive and therefore it has been used as an essential element of water treatment in various European cities (London, Paris, Amsterdam, Stockholm and Zurich) and in many countries of Asia, Africa, South and Central America (Graham 1988; Graham & Collins 1996; Urfer *et al.* 1997; Graham 1999). The slow sand filters that we investigated process water from Lake Zurich that is pre-treated by ozonation, rapid filtration and granular activated carbon filtration. The filters at Zurich are operated under high flow rates and are occasionally designated as *high rate slow sand filters*. Nevertheless, for simplicity we talk about *slow sand filters* throughout this paper.

The infiltration capacity of slow sand filters is seriously limited by clogging processes. Despite the high maintenance costs, regular removal of the upper heavily clogged part of the filter is an efficient method to re-establish a good hydraulic conductivity. The economic efficiency of slow sand filtration may be increased if clogging mechanisms are prevented.

Clogging is defined as the decrease of hydraulic conductivity in a porous medium, and occurs commonly in a wide range of systems (e.g. review in Baveye *et al.* 1998). The progressive augmentation of a medium's physical resistance to water flow results from the reduction in the size of pore space. The mechanisms responsible for these changes are usually classified into physical, chemical and biological factors or a

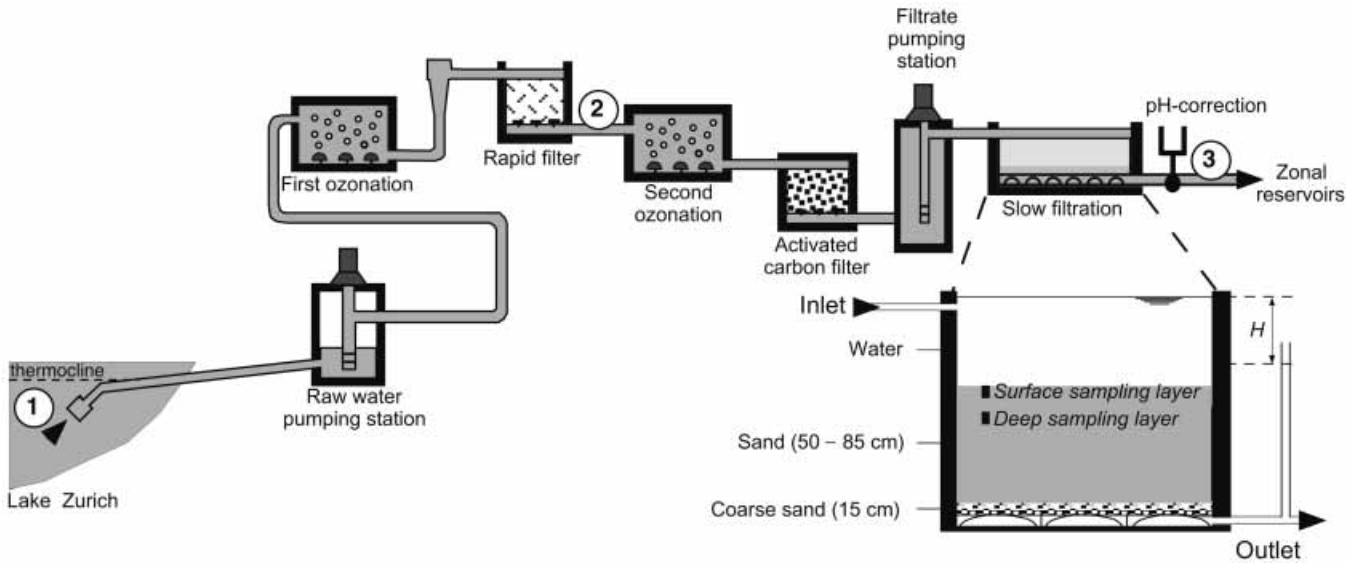

Figure 1 | Water plant of Zurich-Lengg with a detailed profile of the slow sand filters. Sampling layers are indicated in italics. *H* is the total head loss throughout the filter.

combination thereof (Weber-Shirk & Dick 1997*b*; Baveye *et al.* 1998).

Biological processes can be the major reason for clogging and they have been extensively studied in laboratory experiments (e.g. Taylor & Jaffé 1990; Vandevivere & Baveye 1992*b*; Kildsgaard & Engesgaard 2002; Thullner *et al.* 2002*b*). However, the majority of field studies on clogging did not investigate hydraulic conductivity because soil heterogeneities make this measurement difficult. Field determinations of hydraulic conductivity were only made for confined systems such as ponds (Chang *et al.* 1974; Wood & Bassett 1975; Siegrist 1987). Although it was possible to monitor the water infiltration rate, it was not possible to locate clogging processes in the sediment profile.

In the present study, we investigated the change of hydraulic conductivity in slow sand filters of a drinking water plant in Zurich, Switzerland. Physical, chemical and biological parameters potentially related to the decrease of hydraulic conductivity were investigated in the slow sand filters at different stages in the evolution of clogging. Microbial abundance, microbial activity and extracellular polymeric substances (EPS) were quantified to elucidate the contribution of biological parameters to clogging.

SITE DESCRIPTION AND SAMPLING

Major steps of water treatment

Raw water is collected in Lake Zurich at a depth of 30 m (>15 m below the thermocline) and pumped to the Lengg indoor water treatment plant. The different stages of water treatment are shown in Figure 1, and the water quality within the system is summarised in Table 1. A first ozonation (1.1 mg O_3 l^{-1}, ± 25%) is used for disinfection, oxidation and flocculation aid prior to the treatment by rapid sand filters. These filters, made of pumice and quartz sand, remove more than 95% of the particle load. Before activated carbon filtration a second ozonation (0.5 mg O_3 l^{-1}) is conducted. For the mechanical and especially for the biological superfine cleaning, slow sand filters are used (Figure 1). The filters are constructed on top of a floor of special bricks that serve as a drainage area. The filters consist of four layers with increasing grain size from the top to the bottom: a layer of fine sand (50–85 cm), a layer of coarse sand (5 cm), a layer of fine gravel (5 cm) and a layer of gravel (5 cm). The thickness of the fine sand layer varied according to the number of cleaning cycles (removal of the top 5 cm). Thus, the total

Table 1 | Physical and chemical characteristics of the water along the treatment process (numbers refer to the location on Figure 1). Averages and standard deviations for the year 2000 from monthly measurements of Zurich Water Supply

	Location		
Parameter	**Lake water (1)**	**After rapid filtration (2)**	**Before distribution (3)**
Ammonium-N (μM)	0.3 ± 0.19^a	0.2 ± 0.11^b	0.1 ± 0.05^a
Nitrate-N (μM)	54.6 ± 3.39^a	57.6 ± 2.68^b	59.1 ± 2.89^a
Nitrite-N (μM)	0.1 ± 0.08^a	0.0 ± 0.02^b	0.0 ± 0.02^a
Phosphate-P (μM)	0.2 ± 0.12^a	0.3 ± 0.16^b	0.3 ± 0.14^a
Sulphate-S (μM)	153.6 ± 1.8^a	154.2 ± 2.0^b	154.3 ± 2.1^a
Dissolved oxygen (mg l^{-1})	8.4 ± 1.67^a	15.7 ± 1.50^b	14.4 ± 0.84^a
Dissolved organic carbon (mg l^{-1})	1.2 ± 0.06^a	1.0 ± 0.04^b	0.7 ± 0.05^a
pH	7.8 ± 0.13^a	7.7 ± 0.09^c	8.0 ± 0.06^a
Total hardness (mM)	1.4 ± 0.01^a	1.4 ± 0.01^c	1.5 ± 0.03^a
Temperature (°C)	5.8 ± 0.69^a	5.8 ± 0.66^b	5.8 ± 0.69^a

$^a n=12$, $^b n=23$, $^c n=22$.

thickness of the slow sand filter varies between 100 and 65 cm. After 10 to 15 years the remaining sand in a filter must be removed and cleaned. The plant Lengg has 14 slow sand filters (operating in parallel) designated as SSF1 to SSF14. All filters are operated indoors in the dark at 4 to 8°C. Each filter has an area of 1,120 m^2 and a maximum daily load capacity of around 16 $m^3\ m^{-2}$. They are kept at constant water level. The whole system is capable of treating 250,000 $m^3\ day^{-1}$.

Hydraulic behaviour

To study clogging processes, two filter types defined as highly and less clogged were sampled. The highly clogged filters (C +) are filters with a running time of more than 9 years with fast cleaning cycles of 2 to 3 years (Figure 2). These filters had an average hydraulic conductivity around 0.5 m h^{-1} at the sampling dates (Table 2). The less clogged filters (C −) have been running for less than 8 years, have never been cleaned and were only partially clogged at the sampling dates with respect to the C + filters. The dynamics of the system can be visualised by the hydraulic behaviour of the slow sand filters (Figure 2). Newly constructed filters (clean sand) exhibit an initial hydraulic conductivity of about 4 to 7 m h^{-1}. During the following years, the hydraulic conductivity decreases gradually to 0.5 m h^{-1}, indicating the increasing clogging of the system. At this point, filters are drained and cleaned by removing the first 5 cm of the sand. Cleaning raises the hydraulic conductivity by 1 to 2 m h^{-1} for up to three years. However, this method does not restore the original infiltration capacity.

Sampling procedure

Samples were collected on three dates: 2 November 2000, 20 March 2001 and 17 May 2001. The last two sampling dates were chosen before and after lake stratification. For each filter type (C + and C −), three different filters were selected. Samples of sand and interstitial water were taken

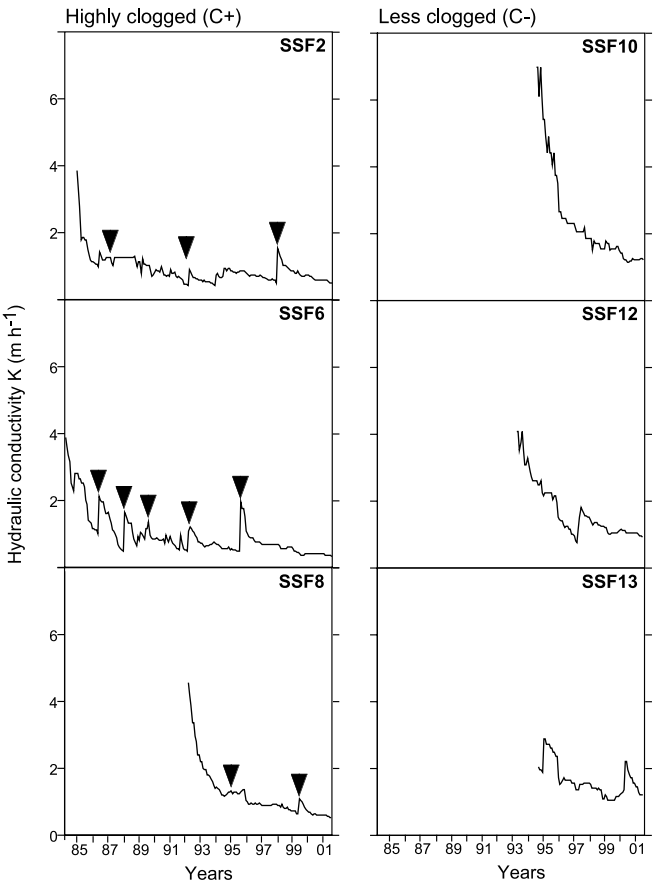

Figure 2 | Evolution of hydraulic conductivity for highly and less clogged filters based on measured head differences from inlet to outlet with a constant water flow of 500 m^3 h^{-1}. Arrows indicate cleaning by removing the top 5 cm of sand.

for each filter at 3 points spaced approximately 1 m apart, forming an equilateral triangle. The triplicate samples of each filter were pooled for subsequent analyses. Interstitial water was collected using porous candles (length 50 mm, diameter 15 mm) placed at 0–5 cm and 15–20 cm below the surface of the sand. Sand was collected by coring with a plexiglass tube (diameter 50 mm). The cores were separated, and two parts (0–5 cm and 15–20 cm) were preserved in an icebox for later analysis. The top layer (0–5 cm) corresponded to the sand removed when slow sand filters are cleaned. Analysis of fine sand profiles (0–1 cm, 1–2 cm, 2–3 cm, 3–4 cm, 4–5 cm) revealed that microbial products (polysaccharides, proteins and cells) and activities were maximal between 1 and 2 cm (data not shown). Differences in the first 5 cm were relatively small and never exceeded 30% of the maximum value. Preliminary measurements of profiles of polysaccharides content and bacterial numbers showed no significant change below 10 cm (data not shown).

METHODS

Measurements of interstitial water characteristics

All chemical and biological analyses were performed using nanopure water (MilliQ), and acid washed glass material. Nitrate, sulphate and phosphate in interstitial water were quantified using an ion chromatograph (Dionex DX-100). Dissolved organic carbon (DOC) was measured with a Total Carbon Analyzer (TOC-5000, Shimadzu) after removing the inorganic carbon with hydrochloric acid (2M, 1 μl ml^{-1}) and stripping with oxygen for 10 min. Refractory dissolved organic carbon (RDOC) was measured as the remaining fraction after 20 days of incubation with the natural bacterial consortia at 20°C (Servais *et al.* 1987). The biodegradable organic carbon (BDOC) fraction was calculated as DOC minus RDOC. The amount of fine particles in the inlet water was measured by filtering 25 l of water with a 0.2 μm filter (Supor) and calculating the increase in weight.

Physical and chemical parameters

Hydraulic conductivity (K) of the entire filter was estimated by measuring the difference in water level between the inlet and outlet of each filter at a constant flux rate of 500 m^3 h^{-1}. To investigate the change of K with increasing depth, piezometers were placed at approximately 1, 2, 3, 4, 5, 10, 15, 20, 30, 50 and 80 cm below the sand surface. The hydraulic conductivity was determined by measuring the piezometric head profile by using Darcy's law:

$$\frac{Q}{A} = K \cdot \frac{\Delta H}{\Delta z} \quad (1)$$

where Q is the flow rate, A is the surface of the slow sand filter, H is the head loss, and z is the depth below the sand

Table 2 | Maintenance and average hydraulic conductivity of the slow sand filters

			Hydraulic conductivity (m h^{-1})		
	Beginning of operation	**Last cleaning***	**November 2000**	**March 2001**	**May 2001**
Highly clogged filters (C +)					
SSF2	June 1985	October 1997	0.60	0.52	0.50
SSF6	October 1984	July 1995	0.37	0.32	0.31
SSF8	June 1992	April 1999	0.57	0.51	0.51
Less clogged filters (C −)					
SSF10	August 1994		1.24	1.28	1.24
SSF12	June 1993		1.00	0.93	0.88
SSF13	October 1994		1.54	1.20	1.20

*By removing the first 5 cm of sand.

surface. Measurements were conducted at different flow rates (500 and 150 m^3 h^{-1}) to verify that computed K values were constant.

Grain size distribution of the sand was determined for dried sand from the top 5 cm that was separated with a sieve series (0.063, 0.125, 0.25, 0.5 and 1 mm). Sieving was performed until each size class comprised at least 10 g of dry sand. Water content was measured by loss of weight after drying (24 h at 60°C) and porosity was determined gravimetrically. In the sand carbon is present as total organic matter (TOM) or calcite. TOM of the sand was measured by loss of weight after ignition (4 h at 550°C; Bretschko & Leichtfried 1987) of 10 g of dry sand. Calcite content of the sand was estimated as the carbon content of burned samples (4 h at 550°C) measured with a carbon analyser (CHNS-932, Leco).

Polysaccharide and protein quantification

Polysaccharides were quantified within four hours of sampling using the Dubois method (Dubois *et al.* 1956). Sonication (2 min, power 7, Sonifer B-12 Branson) was applied to detach the polysaccharides from 10 g of wet sand placed in 50 ml of water (Mermillod-Blondin *et al.* 2001). An aliquot (0.5 ml) of the supernatant was mixed with phenol solution and 95% sulphuric acid, and incubated at room temperature in the dark for 1 h. Absorbance was measured at $\lambda = 495$ nm with a photometer (Uvikon, Kontron Instrument). Polysaccharide content was expressed as mg of glucose equivalent per gram of dry sand.

Proteins, extracted by the same sonication procedure, were quantified using the Lowry method (Lowry *et al.* 1951). Protein content was expressed as mg of bovine serum albumin (BSA) equivalent per gram of dry sand.

Bacterial abundance and volume

Number of total bacteria were counted using DAPI (4′,6-diamidino-2-phenylindol) staining (Porter & Feig 1980). Wet sand (1 g) fixed with formaldehyde (final concentration: 4%) was diluted with 100 ml 0.1% pyrophosphate. Bacteria were detached by sonication as described previously, and aliquots were spotted on to slides and stained with DAPI solution (Schönholzer *et al.* 1999). The slides were examined at 400 × magnification

with a microscope (Zeiss Axiophot Plan Neofluar) fitted for epifluorescence measurements with a 50 W high pressure mercury bulb and a filter set 02 (Zeiss, FT395, LP420). At least 40 randomly selected fields per triplicate measurement were counted. The number of bacteria was expressed per gram of dry sand.

Bacterial volumes were analysed in samples from May by image analysis of five images per triplicate with up to 100 cells per image (Schönholzer *et al.* 2002). Cell volumes were determined based on measurements of area and perimeter for each organism or bacterial agglomerate (Bloem *et al.* 1995; Russ 1995). Volume of bacterial cells was expressed as percentage of pore space.

Bacterial activity

Numbers of ETS-active bacteria (i.e. bacteria with an active electron transport system) were measured using CTC (5-cyano-2,3-ditolyl tetrazolium chloride) staining (Rodriguez *et al.* 1992). Wet sand (1 g) was incubated for 3 h in the dark at room temperature with 1 ml CTC solution (1.4 mg ml^{-1}). The reaction was stopped by adding 0.25 ml of 7% formaldehyde. Samples were stored at −20°C before analysis. Samples were diluted with 50 ml 0.1% pyrophosphate, and bacteria were detached from the sand particles by sonication as previously described. Ten μl aliquots were spotted on to slides. The preparations were allowed to air dry, and slides were mounted with Citifluor. The preparations were examined at 400× magnification as described above with the filter set Hq Cy3 (FT 560, BP 575-640). At least 40 randomly selected fields were counted per triplicate measurement. The number of ETS-active bacteria was expressed per gram of dry sand. Percentage of ETS-active bacteria was calculated by dividing the abundance of ETS-active bacteria by total number of bacteria determined by DAPI staining.

Hydrolytic activity

Hydrolytic activity of microorganisms was measured using fluorescein diacetate (FDA) as a substrate for hydrolases (Fontvieille *et al.* 1992). Wet sand (1 g) was incubated in 3 ml of phosphate buffer (pH = 7.6) with 0.1 ml of FDA solution (2 mg ml^{-1}) and kept at 20°C and darkness until the green colour of the fluorescein was visible (0.5–2 h). The reaction was stopped by addition of 3 ml of mercuric chloride solution (200 mg l^{-1}). The supernatant was filtered (0.45 μm, HAWP Millipore), and absorbance of the solution was measured at $\lambda = 490$ nm. Results were expressed as μmoles of FDA hydrolysed per hour and gram of dry sand.

Data analysis and statistical methods

Results are averages of measurements made in three filters of each type (C+ or C−) ± standard errors. Spatial and seasonal variations of parameters were examined using the Tukey test (multiple comparison procedure) and analysis of variance (ANOVA) after checking normality and homoscedasticity (Statview 4, Abacus). Spatial variations for each sampling season were tested using ANOVA2 (filter type × sampling depth) by grouping data from the three filters of each type. Temporal variation was investigated by ANOVA1 (date) for each combination of filter type and sampling depth.

For the determination of biovolumes we assumed that with the exception of polysaccharides and proteins other types of microbial substances can be neglected. Volumes of biomass extracted by sonication from the sand were calculated by using the amount of polysaccharides and proteins, and reported biofilm densities, which range from 5 to 130 kg dry mass m^{-3} wet volume (Christensen & Characklis 1990). Volume of biomass was expressed as percentages of pore space.

RESULTS

Physical and chemical properties of water

Interstitial water had similar chemical characteristics in all filters (Figure 3). The average of all interstitial water samples was 57.6 ± 4.6 μM for nitrate, 163 ± 10 μM for sulphate and 3.4 ± 0.4 mg l^{-1} for BDOC. Water chemistry changed little during the infiltration and showed few

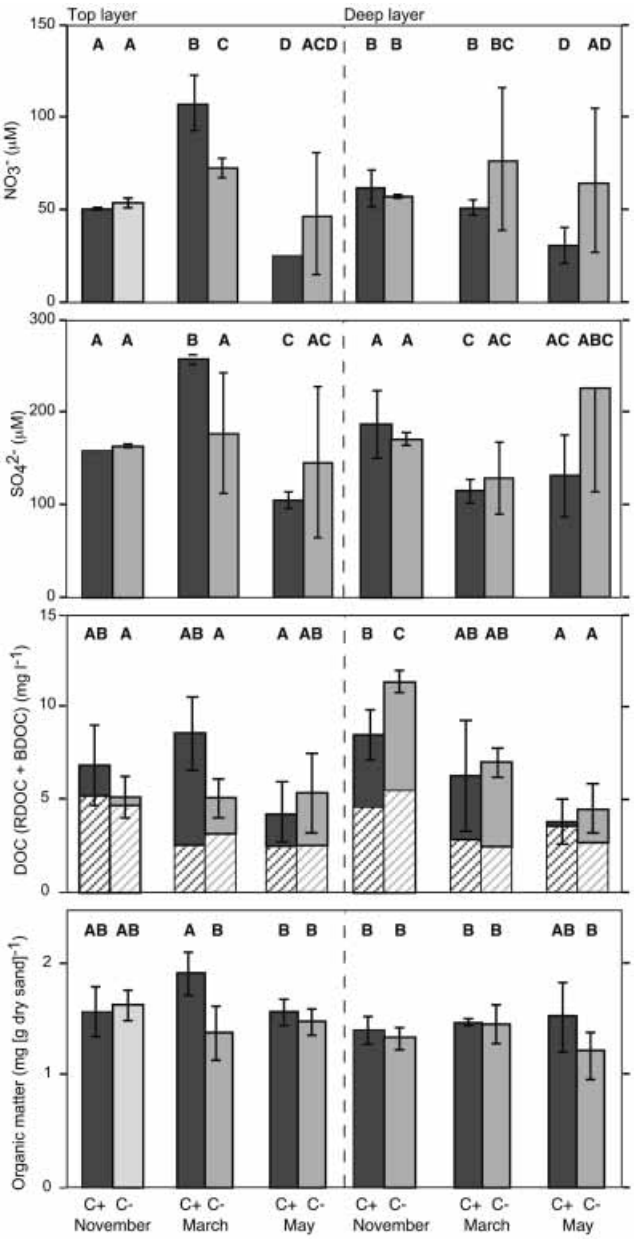

Figure 3 | Chemical characteristics of interstitial water of the top (0–5 cm) and deep (15–20 cm) layers of the two filter types: highly clogged (C+, dark grey) and less clogged (C−, pale grey). Bars identified by different letters are significantly different (Tukey test, 5%).

temporal changes. The inlet water contained a mean of 0.4 mg l^{-1} of fine particles (Table 3).

Detailed statistical analyses of data given in Figure 3 are presented in Table 4. In November, nitrate and DOC concentrations showed significant changes during infiltration, which were significantly higher in the deep layer compared with the top layer (Figure 3). Nitrate and sulphate concentrations were significantly higher in the top layer of C+ filters in March compared with other sampling dates, whereas DOC was significantly lower in the deep layer of C− filters in May compared with November. The concentration of fine particles in the inlet water showed relatively high variations within the measured filters. Nevertheless, the average amount of particles was not statistically different according to the filter type (Table 3).

Physical and chemical properties of the filter matrix

Most of the observed clogging occurred in the first centimetres of infiltration demonstrated by a dramatic head loss in those layers (Figure 4). Average hydraulic conductivity was calculated using Darcy's law where ($\Delta H/\Delta z$) was given by the slope of linear regression of head loss vs. depth for defined layers. K was calculated from points in three layers from approximately 0–10, 10–50 and 50–80 cm below sand surface, with values of 0.24, 1.42 and 8.49 m h^{-1} in the C− filter, and 0.09, 0.87 and 6.66 m h^{-1} in the C+ filter, respectively (Figure 4). K increased by a factor of 6–10 from one layer to the next. The C+ filter showed smaller conductivities in all respective layers. The sand of the upper part of all filters exhibited a similar grain size distribution and a similar amount of calcite (Table 3). Calcite content was around 6% of the weight of sand and depicted no trend in C+ or C− filters. Pore volume per weight of dry sand was calculated based on the average of porosity measurements (0.21) and bulk density of sand (2.87 kg l^{-1}). The total volume occupied by 1 g of dry sand was 0.44 ml, with 0.35 and 0.09 ml for sand matrix and pore space, respectively.

Biological properties of the filter matrix

Temporal pattern

Biological characteristics are shown in Figures 5 and 6, detailed statistical analyses of these data are presented in Table 4. Polysaccharide content depicted small temporal

Table 3 | Particle content of inlet water, and grain size distribution and calcite content of fine sand layer

	Highly clogged filters (C+)				Less clogged filters (C−)			
	SSF2	SSF6	SSF8	Mean±stdev	SSF10	SSF12	SSF13	Mean±stdev
Water								
Fine particles	Content of fine particles (> 0.2 μm) in the inlet water (mg l^{-1})							
	1.08	0.44	0.25	0.87 ± 0.91	0.44	0.09	0.14	0.22 ± 0.19
Sand								
Grain size diameter (0–20 cm)	Grain size distribution expressed as cumulative percentage of the dry sand							
< 63 μm	0.15	0.24	0.04	0.14 ± 0.11	0.11	0.16	0.03	0.10 ± 0.08
< 125 μm	0.44	0.47	0.20	0.37 ± 0.17	0.31	0.48	0.35	0.38 ± 0.10
< 250 μm	5.82	5.52	3.12	4.82 ± 1.68	6.18	2.38	5.67	4.74 ± 2.33
< 500 μm	46.51	52.50	45.30	48.10 ± 4.36	67.08	34.91	55.72	52.57 ± 4.46
< 1000 μm	93.12	84.14	90.44	89.23 ± 5.21	94.55	74.12	88.01	85.56 ± 8.81
Depth	Calcite content of the sand (mg [g dry sand]$^{-1}$)							
Top layer (0–5 cm)	58.70	59.0	79.60	65.7 ± 12.0	61.80	60.20	64.50	62.1 ± 2.21
Deep layer (15–20 cm)	38.0	59.70	61.70	53.1 ± 13.1	41.80	66.0	83.0	63.6 ± 20.7

variations with highest values in November (Figure 5). This trend was present for both filter types and sampling depths, but was significant only for the top layer of the C+ filters and the deep layer of C− filters. In the top layer of C− filters the polysaccharide content shows a tendency to decrease. Most of the measured biological characteristics changed significantly according to the sampling date (Table 4). Protein content displayed a similar trend throughout the sampling period for both filter types (Figure 5). In the top layer of C+ filters protein content was significantly lower in November than in March and May, while protein content in the top layer of the C− filters increased continuously from November to May. In the deep layer of C+ and C− filters maximal values were recorded in March.

Bacterial abundance increased from November to May for both filter types and sampling depths (Figure 6). Bacterial abundance rose in the top layer from 2×10^8 cells [g dry sand]$^{-1}$ in November to 1.9×10^9 cells [g dry sand]$^{-1}$ in May; in the deep layer from 2×10^8 cells [g dry sand]$^{-1}$ in November to 1.5×10^9 cells [g dry sand]$^{-1}$ in May. Growth was especially evident in the 2 months between the March and the May sampling compared with the 4.5 months between the November and March sampling. Number of ETS-active bacteria showed a different temporal pattern (Figure 6). In the top layer bacterial activity was maximal in March, whereas in the deep layer bacterial activity increased from November to March and remained at that level in May. Because bacterial abundance and activity had different temporal patterns, the fraction of ETS-active bacteria of total number of bacteria varied between sampling dates: 9.4 ± 1.4% in November, 12.7 ± 1.9% in March, and 2.4 ± 0.3% in May.

Table 4 | Statistical differences of chemical and microbial characteristics between sampling depths, dates, filter types (higly clogged C+, and less clogged C−) and depths tested by ANOVA 1 and 2

	ANOVA2 (filter type×depth)								ANOVA1 (dates)			
	All dates		November		March		May		C+		C−	
	Filter type	Depth	Filter type	Depth	Filter type	Depth	Filter type	Depth	Top layer[a]	Deep layer[b]	Top layer	Deep layer
Chemical characteristics												
Nitrate	0.4427	0.7878	0.8283	0.0481*	0.7116	0.0796	0.1404	0.5084	0.0002***	0.0271*	0.3708	0.7794
Sulphate	0.6597	0.7256	0.5971	0.1382	0.2359	0.0571	0.1791	0.2645	<0.0001***	0.1290	0.8249	0.3602
Dissolved organic carbon (DOC)	0.6319	0.1830	0.5571	0.0049**	0.3527	0.9144	0.8838	0.7141	0.3757	0.3071	0.9828	0.0018**
Refractory DOC	0.7987	0.9447	0.9202	0.9590	0.8872	0.7855	0.7145	0.9729	0.2550	0.2473	0.5506	0.1652
Biodegradable DOC	0.9936	0.4417	0.2725	0.3112	0.2908	0.9850	0.7565	0.6927	0.0783	0.9064	0.5530	0.1633
% Biodegradable DOC	0.6018	0.6445	0.2215	0.7119	0.7635	0.9786	0.7549	0.9234	0.0149*	0.9504	0.6188	0.3887
Total organic matter	0.9277	0.1457	0.6794	0.1830	0.9442	0.1828	0.6871	0.4596	0.0657	0.6405	0.4150	0.4333
Biological characteristics												
Polysaccharides	<0.0001***	<0.0001***	0.0234*	0.0008**	0.0014**	0.4250	0.0432*	0.0013**	0.0206*	0.0923	0.1096	0.0148*
Proteins	0.0052*	<0.0001***	0.0158*	0.0212*	0.0463*	0.0018**	0.4270	<0.0001***	0.0059*	0.0095*	0.0013*	0.0002***
Total bacteria	0.5243	0.0017**	0.7788	0.0806	0.6960	0.0018**	0.2900	0.0319*	<0.0001***	<0.0001***	0.0002***	0.0004***
ETS-active bacteria	0.0290*	<0.0001***	0.3141	0.0102*	0.0333*	<0.0001***	0.0988	0.4533	0.0003***	0.0288*	0.0017**	0.0261*
% of ETS-active bacteria	0.0997	0.0093*	0.0683	0.0040*	0.0559	0.0041**	0.1492	0.5945	0.0004***	0.0633	0.0343*	0.0081*
Hydrolytic activity	0.1708	<0.0001***	0.4635	0.1378	0.0870	0.0027**	0.9949	0.0003***	0.0223*	0.0029**	0.0102*	0.7870
Pore space occupied	0.0056*	<0.0001***	0.0054*	0.0010**	0.0162*	0.0610*	0.1396	<0.0001***	0.2241	0.0234*	0.0452*	0.0003***

P-values: *p<0.05, **p<0.005, ***p<0.0005.
[a]0–5 cm, [b]15–20 cm.

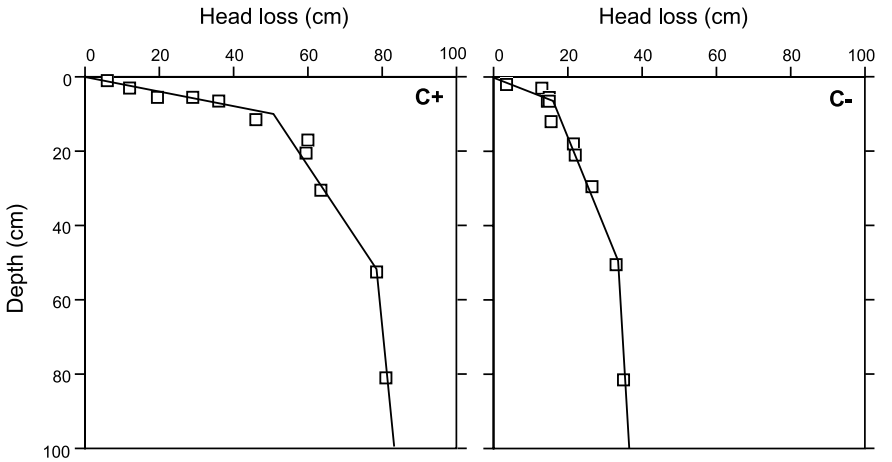

Figure 4 | Depth profile of the head loss for filters SSF2 and SSF10 as representatives of C+ and C− filters, respectively, based on measurement of piezometric levels in August 2001.

The pore space occupied by EPS (proteins and polysaccharides) was calculated as the minimum volume by using the highest density reported in the literature (130 kg m^{-3}, Christensen & Characklis 1990). Pore space occupied by EPS (Table 5) did not change much according to the sampling date in the top layer of the C+ filters. In the top layer of C− filters EPS occupied an increasing percentage of the pore space over time. The percentage of occupied pore space almost doubled in the 6.5 months from November till May. The almost fourfold increase of protein content accounted for this change. In the deep layer EPS occupied the same pore space in November and in May, but surprisingly, significantly more pore space was occupied in March. Between March and May the pore space occupied by EPS in the deep layer decreased by about 50% for both filter types. The volume of bacteria cells was minuscule compared with the volumes of EPS (Table 5).

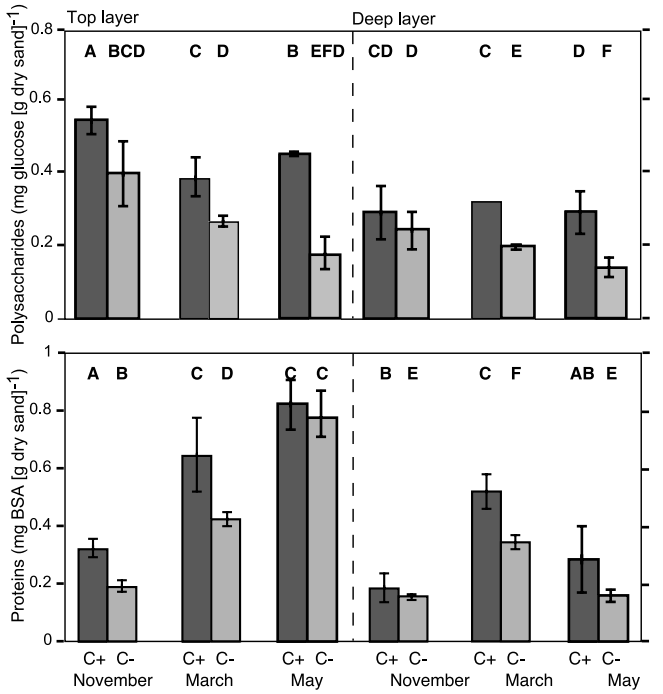

Figure 5 | EPS produced by microorganisms of the top (0–5 cm) and deep (15–20 cm) layers of the two filter types: highly clogged (C+, dark grey) and less clogged (C−, pale grey). Bars identified by different letters are significantly different (Tukey test, 5%).

Spacial pattern

All biological characteristics, EPS (Figure 5), bacterial abundance and activity, number of ETS-active bacteria and hydrolytic activity (Figure 6) significantly changed with sampling depth. For both filter types all biological characteristics were significantly higher in the top layer (Table 4). Biomass (bacterial cells, polysaccharides and proteins) occupied an average of 6–14% of the pore space of the top layer and an average 3–9% of the pore space of the deep layer (Table 5). Differences between filter types

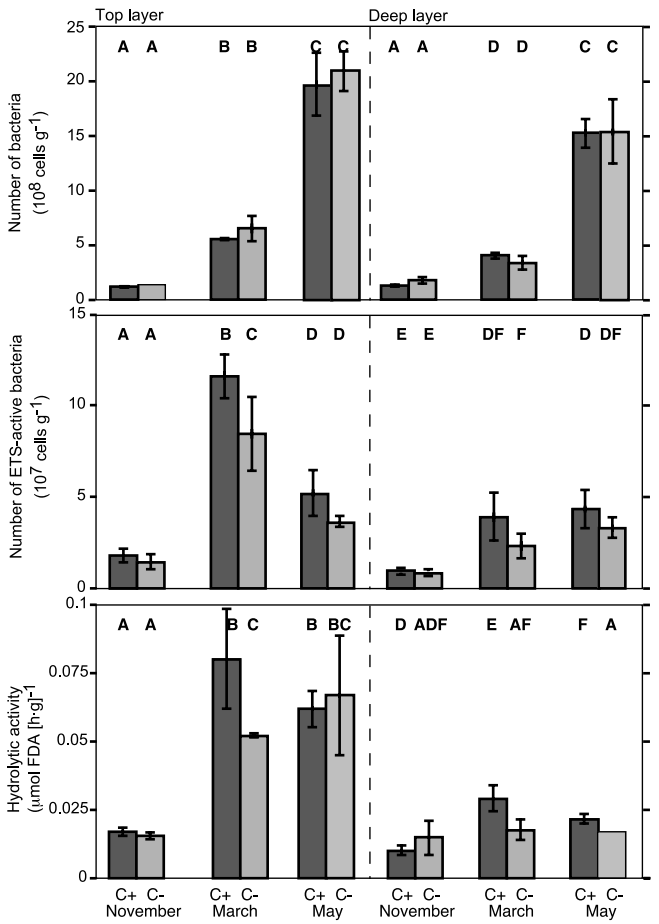

Figure 6 | Microbial characteristics of the top (0–5 cm) and deep (15–20 cm) layers of the two filter types: highly clogged (C+, dark grey) and less clogged (C−, pale grey). Bars identified by different letters are significantly different (Tukey test, 5%).

were less pronounced, but some were significant especially in the top layer. C+ filters contained significantly more EPS than C− filters, except the protein content in the top layer in May. C+ filters also showed higher activity (number of ETS-active bacteria and hydrolytic assay) in March and higher bacterial abundance in May than the C− filters (Table 4).

DISCUSSION

Hydraulics

The average hydraulic conductivity of all sand filters exhibited a strong decrease over time (Figure 2). The initial values of the hydraulic conductivity were between 4 and 7 m h^{-1}. This is only slightly higher than the theoretically predicted value of 3 m h^{-1} using the Kozeny-Carman equation in a version given in Bear (1972):

$$K=\frac{\rho g}{\mu}\cdot\frac{d^2 n}{180(1-n)^2} \quad (2)$$

with $d=1$ mm as the typical grain diameter and $n=0.21$ as porosity. ρ is the density of water, g the gravitational acceleration and μ the dynamic viscosity of water. This indicates that the initial hydraulic conductivity of the sand filter was determined by the sand matrix only. Because of the approximately homogeneous packing of the fine sand layer, it can be assumed that the initial hydraulic conductivity of this layer did not vary with depth. Measurement of the piezometric head profile and thus the hydraulic conductivity along the depth of the sand filters revealed that the fine sand layer of a clogged sand filter could be divided into three sub-layers (Figure 4), each with a different development of hydraulic conductivity over time. The uppermost layer, with a thickness of approximately 5–10 cm, showed the highest reduction of hydraulic conductivity, but in the second layer, which ends at a depth of approximately 50 cm, a reduction of hydraulic conductivity could also be observed. Below a depth of 50 cm the measured hydraulic conductivity was actually slightly higher than the average hydraulic conductivity of a newly built filter, suggesting that the hydraulic conductivity in this layer did not change over time.

The varying extent of clogging depending on the layer explains the effect that the removal of the top 5 cm of a sand filter has on the average hydraulic conductivity. The top 5 cm constitutes the most clogged part of a filter. After removal, the average hydraulic conductivity of the sand filters increased to 1–2 m h^{-1}, similar to the values measured for the second layer from 10–50 cm depth. As we observed no changes of hydraulic conductivity with depth within each of these layers, it is likely that clogging processes proceed homogeneously within each layer. Thus, samples taken from a certain depth were assumed to be representative for the entire respective layer. In particular, samples taken from the top 5 cm represented the top layer (0–10 cm depth) and samples taken at a depth of

Table 5 | Calculation of the percentage of pore space occupied by bacteria, proteins and polysaccharides

		Microbial substances[b]		
	Bacterial cells[a]	Proteins	Polysaccharides	Total
Top layer				
Highly clogged C +				
November	0.01 ± 0.001	4.2 ± 0.70	5.8 ± 0.57	10.0 ± 1.27
March	0.05 ± 0.002	8.4 ± 0.19	4.1 ± 0.62	12.5 ± 0.81
May	0.16 ± 0.034	8.7 ± 0.12	4.8 ± 0.28	13.6 ± 0.40
Less clogged C −				
November	0.01 ± 0.001	2.4 ± 0.88	4.1 ± 0.86	6.5 ± 1.74
March	0.05 ± 0.001	6.8 ± 0.99	2.8 ± 0.35	9.6 ± 1.34
May	0.17 ± 0.037	8.9 ± 0.18	3.1 ± 0.84	12.0 ± 1.02
Deep layer				
Highly clogged C +				
November	0.01 ± 0.002	2.5 ± 0.49	3.1 ± 0.95	5.6 ± 1.43
March	0.03 ± 0.004	5.6 ± 0.51	3.6 ± 0.32	9.2 ± 0.83
May	0.12 ± 0.018	3.0 ± 0.16	1.9 ± 0.99	4.9 ± 1.17
Less clogged C −				
November	0.01 ± 0.004	1.1 ± 0.11	2.6 ± 0.71	3.8 ± 0.88
March	0.03 ± 0.007	4.5 ± 0.42	3.0 ± 0.68	7.5 ± 1.11
May	0.12 ± 0.033	1.6 ± 0.36	1.5 ± 0.51	3.2 ± 0.87

[a]Bacterial volume was based on the average biovolume of May samples (0.06 mm^3 $cell^{-1}$).
[b]To calculate the minimum volume occupied by proteins and polysaccharides, the highest density reported in literature was used (130 kg m^{-3}, Christensen and Characklis 1990).

15–20 cm represented the deeper layer from 10 to 50 cm depth.

Clogging due to physical and chemical causes

To verify whether the particles suspended in the infiltrating water were contributing to the clogging of the sand filters, the measured particle mass had to be transferred into a volume. As we could not find any reason for the differences between the particle concentrations measured for the individual filters, we assumed this fluctuation to be a random process. To estimate the maximal potential impact of the particle deposition on the clogging of the filters, we used a particle concentration of 1 mg l^{-1}, which

is approximately equal to the highest measured particle concentration for an individual filter (but higher than the average for the C+ and C− filters). Assuming this concentration of particles with the same density as sand and an average flow rate of 150 m^3 h^{-1}, a volume of 38 l of particles entered each filter every month.

Supposing that all these particles were deposited within the top layer of 10 cm thickness and that the deposition had a porosity of 0.3, the total pore space in the top layer would have been reduced by 7% during the typical period of 2.5 years between two cleaning cycles. In this case particle deposition would have contributed to the clogging of the top layer of the sand filters but not to the clogging of the deeper layers. Thus, the clogging of the deep layers would have been due to other processes than particle deposition. In contrast, assuming that the particle deposition took place homogeneously in the top and the deep layers, a pore volume reduction of only 1 to 2% would result in 2.5 years. In this case particle deposition would not have caused major clogging effects, mainly because large pores may still retain their full water carrying capacity (Goldenberg *et al.* 1993). Because these calculations were based on particle concentrations higher than the measured averages, it is likely that the porosity reductions, and thus the clogging, caused by particle deposition in the filters were even smaller than the values calculated above. The average particle concentration was different for each filter type, but due to the high standard deviations, this difference was not statistically significant. Therefore, the changes in the clogging behaviour of the two filter types were not attributed to differences in particle deposition.

Water with a calcium content of approximately 1.3 mM, such as water from Lake Zurich, may support some calcite precipitation, which contributes to the clogging of sand filters (Weber-Shirk & Dick 1997*a*). In the present study we observed that calcite contributed to the weight of the sand grains by approximately 6%. Assuming that the density of the sand was not changed due to the calcite, 6% of the sand volume was composed by calcite. In case that the calcite was built during the operation of the filters, calcite precipitation may have caused a reduction of the hydraulic conductivity of the filters. Potential clogging due to calcite precipitation was considered to occur uniformly along the depth of the filters because the measured calcite content and the grain size distribution were similar in all samples. Therefore, we infer that calcite precipitation was not the cause for the different degree of clogging in the different layers of the sand filters.

Clogging due to biological causes

Biological activities in the sand filters were in the same range as reported values for comparable natural environments such as aquifers with river water infiltration (Mauclaire *et al.* 2000; Mauclaire & Gibert 2001). As a consequence of biological activity, the produced biomass reduced the pore space of the sand filters. The volume of bacterial cells did not exceed 0.2% of the pore volume, but the EPS produced by the bacteria occupied at least 7% of the top layer and 3% of the deep layer of the sand filters. The sand filters in the Lengg plant were operated in the dark and no algae were found in the pore space. In column experiments (e.g. Vandevivere & Baveye 1992*b* and results reviewed in Vandevivere *et al.* 1995) it has been reported that the hydraulic conductivity of sand can be reduced by up to three orders of magnitude because of biomass, which occupies only a small fraction of the pore space. This was theoretically explained by assuming that biomass preferentially plugged the bottlenecks of the water flow (Thullner *et al.* 2002*a*).

In addition, it must be emphasised that the EPS volumes presented in this study were determined using a density of 130 g l^{-1}. This calculation of biovolume is strongly driven by the conversion factor used for EPS density. Values reported in literature range from 5 to 130 kg m^{-3} (Christensen & Characklis 1990). In order to be stringent in our conclusions we calculated a minimum biomass volume by using the maximum biofilm density reported. So biovolumes tended to be underestimated on the whole and, consequently, the occupied pore space was potentially much larger. The finding that the majority of the biomass was composed of EPS agrees with other studies that investigated bioclogging of porous media (Vandevivere & Baveye 1992*a*; Thullner *et al.* 2002*b*). These studies attributed the observed clogging effects to the EPS produced by the bacteria, whereas the bacterial cells by themselves were found to have a negligible influence on occupied pore space and hydraulic conductivity.

We observed a decrease of biomass in the deep layer between the sampling in March and in May 2001. During this period the lake becomes increasingly stratified and the phosphate concentration at a depth of 30 m decreases (data not shown). However, given the treatment steps prior to the slow sand filtration (Figure 1) it is questionable whether the observed decrease in biomass is due to changes in the lake water composition.

Another biological activity potentially contributing to clogging of the sand filters is the production of gas by bacteria in excess of the solubility in water. In such cases, the clogging due to gas bubbles may be more important than the clogging due to the biomass (Soares *et al.* 1989). However, we found no indication that gas bubble production occurred in the sand filters. In particular, the high concentration of dissolved oxygen measured in the outflow of the filters suggests that anaerobic processes were negligible. Additionally, nitrate concentration did not change between inflow and outflow of the filters and we could never detect any foul smell during sampling. Thus, nitrogen gas, sulphide or methane production or fermentation were not likely to occur.

Comparison of causes of clogging

Comparing the different causes for the clogging of the sand filters showed that particle deposition, calcite precipitation and biomass production may all have been responsible for the clogging (Figure 7). The extent to which these different causes potentially contributed to the clogging of the filters varied. As calcite precipitation could not explain the different clogging in the top and deep layer, it is not likely that it had a major impact on the hydraulic conductivity of the sand filters in general. Nevertheless, it may have supported the formation of flocs composed of EPS, bacterial cells and minerals, which potentially affect the hydraulic conductivity of the sand matrix (Ali *et al.* 1985; Rinck-Pfeiffer *et al.* 2000). The deposition of particles was shown to potentially contribute to the clogging of the top layer, whereas for the deep layer, particle deposition could not explain the clogging. In contrast, we observed considerable amounts of biomass, which could account for the clogging of the top and the deep layer, even without other clogging processes taking place. According to our measurements and calculations, deposited particles occupied no more than 7% of the pore space, whereas biovolume occupied at least 7%.

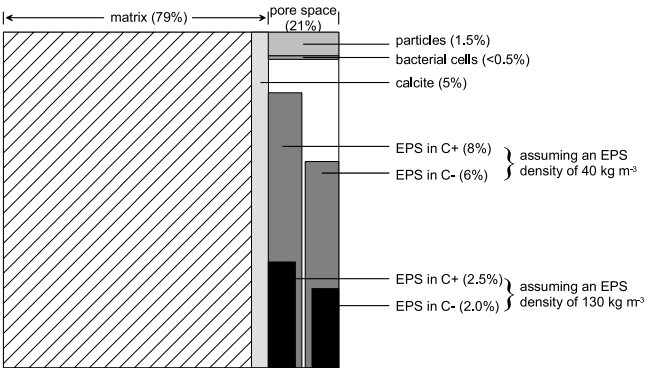

Figure 7 | Schematic composition of a unit volume of the top layer of the sand filters, showing the volume fractions attributed to the individual clogging processes. EPS values are averages of the three sampling dates.

These results indicate that the bioclogging was at least an important if not the major reason for the observed decrease in the hydraulic conductivity of the sand filters (Figure 7). This conclusion agrees with Rice (1974), who inferred that the clogging was mainly due to biological rather than physical and chemical causes for water containing a low concentration of suspended particles, with a slow development of clogging taking place not only in the top centimetres of the filters. Another indication that the observed clogging was mainly attributed to the presence of biomass was the correlation between the amounts of biomass and the different degrees of clogging in the top and deep layers as well as the different degrees of clogging in the two filter types C + and C − (Figure 7).

CONCLUSIONS

Clogging due to microbial activity contributed to a large extent to the total clogging of the sand filters and, on average, at least 10% of the pore space in the top layer was occupied by biomass. The development of clogging in the highly clogged filters (C +) was different from that of the less clogged filters (C −). We were able to demonstrate

that this difference correlated with varying amounts of biomass (particularly extracellular polysaccharides and proteins) found in the two filter types. It appears that the production of these microbial substances cannot be explained solely by environmental variables, suggesting that this process is also controlled at the organism level by the diversity of microbial populations. Build-up of biomass in well-defined systems such as slow sand filters may be a valuable model for exploring how bacterial and faunal diversity and community structure relate to bioclogging. This assumption will be a central topic of future research.

ACKNOWLEDGEMENTS

The authors would like to thank K. Suter and R. Stettler from Zurich Water Supply for their warm welcome and efficient help. Thanks also to E. Kaiser (Swiss Federal Institute for Environmental Science and Technology) and U. Buchs (Zurich Water Supply) for DOC measurements.

ABBREVIATIONS

λ	wavelength
μ	dynamic viscosity of water
ρ	density of water
A	surface of slow sand filter
ANOVA	analysis of variance
BDOC	biodegradable dissolved organic carbon
BSA	bovine serum albumin
C +	highly clogged slow sand filters
C −	less clogged slow sand filters
CTC	5-cyano-2,3-ditotyl tetrazolium chloride
d	grain size diameter
DAPI	4′,6-diamidino-2-phenylindol
DOC	dissolved organic carbon
EPS	extracellular polymeric substances
ETS	electron transport system
FDA	fluorescein diacetate
g	gravitational acceleration
H	head loss
K	hydraulic conductivity
LP	log pass
M	molar
n	porosity
Q	flow rate
RDOC	refractory dissolved organic carbon
SSF	slow sand filter
TOM	total organic matter
z	depth below the sand surface

REFERENCES

Ali, W., O'Melia, C. R. & Edzwald, J. K. 1985 Stability of particles in lakes: measurement and significance. *Wat. Sci. Technol.* **17**, 701–712.

Baveye, P., Vandevivere, P., Hoyle, B. L., DeLeo, P. C. & Sanchez de Lozada, D. 1998 Environmental impact and mechanisms of the biological clogging of saturated soils and aquifer materials. *Crit. Rev. Environ. Sci. Technol.* **28**, 123–191.

Bear, J. 1972 *Dynamics of Fluid in Porous Media*. Elsevier, New York.

Bloem, J., Veninga, M. & Shepherd, J. 1995 Fully automatic determination of soil bacterium numbers, cell volumes, and frequencies of dividing cells by confocal laser scanning microscopy and image analysis. *Appl. Environ. Microbiol.* **61**, 926–936.

Bretschko, G. & Leichtfried, M. 1987 The determination of organic matter in river sediments. *Arch. Hydrobiol.* **68**, 403–417.

Chang, A. C., Olmstead, W. R., Johanson, J. B. & Yamashita, G. 1974 The sealing mechanism of wastewater ponds. *J. Wat. Pollut. Control Fed.* **46**, 1715–1721.

Christensen, B. E. & Characklis, W. G. 1990 Physical and chemical properties of biofilms. In *Biofilms* (ed. Characklis, W. G. & Marshall, K. C.), pp. 93–130. John Wiley & Sons, New York.

Dubois, M., Gilles, K. A., Hamilton, J. K., Rebers, P. A. & Smith, F. 1956 Colorimetric method for determination of sugars and related substances. *Anal. Chem.* **28**, 350–356.

Fontvieille, D., Outaguereouine, A. & Thevenot, D. R. 1992 Fluorescein diacetate hydrolysis as measure of microbial activity in aquatic systems. Application to activated sludge. *Environ. Technol.* **13**, 531–540.

Goldenberg, L. C., Hutcheon, I., Wardlaw, N. & Melloul, A. J. 1993 Rearrangement of fine particles in porous media causing reduction of permeability and formation of preferred pathways of flow: experimental findings and a conceptual model. *Transp. Porous Media* **13**, 221–237.

Graham, N. J. D. 1988 *Slow Sand Filtration: Recent Developments in Water Treatment Technology*. Horwood E., Chichester.

Graham, N. J. D. 1999 Removal of humic substances by oxidation/biofiltration processes- a review. *Water. Sci. Technol.* **40**, 141–148.

Graham, N. J. D. & Collins, R. 1996 *Advances in Slow Sand Alternative Biological Filtrations*. John Wiley & Sons, Chichester.

Kildsgaard, J. & Engesgaard, P. 2002 Tracer and image analysis of biological clogging in two-dimensional flow tank experiments. *Ground Wat. Monit. Remed.* **22** (2), 60–67.

Lowry, O. H., Rosebrough, N. J., Farr, A. L. & Randall, J. R. 1951 Protein measurement with Folin phenol reagent. *J. Biol. Chem.* **193**, 265–275.

Mauclaire, L. & Gibert, J. 2001 Environmental determinants of bacterial activity and faunal assemblages in alluvial riverbank aquifers. *Arch. Hydrobiol.* **152**, 469–487.

Mauclaire, L., Gibert, J. & Claret, C. 2000 Do bacteria and nutrients control faunal assemblages in alluvial aquifers? *Arch. Hydrobiol.* **148**, 85–98.

Mermillod-Blondin, F., Fauvet, G., Chalamet, A. & Creuzé des Châtelliers, M. 2001 A comparison of two ultrasonic methods for detaching biofilms from natural substrata. *Int. Rev. Hydrobiol.* **86**, 349–360.

Porter, K. & Feig, Y. 1980 The use of DAPI for identifying and counting aquatic microflora. *Limnol. Oceanogr.* **25**, 943–948.

Rice, R. C. 1974 Soil clogging during infiltration of secondary effluent. *J. Wat. Pollut. Control Fed.* **46**, 708–716.

Rinck-Pfeiffer, S., Ragusa, S., Sztajnbok, P. & Vandevelde, T. 2000 Interrelationships between biological, chemical, and physical processes as an analogue to clogging in aquifer storage and recovery (ASR) wells. *Wat. Res.* **34**, 2110–2118.

Rodriguez, G. G., Phipps, D., Ishiguro, K. & Ridway, H. F. 1992 Use of fluorescent redox probe for direct visualization of actively respiring bacteria. *Appl. Environ. Microbiol.* **58**, 1801–1808.

Russ, J. C. 1995 *The Image Processing Handbook*. CRC Press, Boca Raton, Florida.

Schönholzer, F., Hahn, D. & Zeyer, J. 1999 Origins and fate of fungi and bacteria in the gut of *Lumbricus terrestris* studied by image analysis. *FEMS Microbiol. Ecol.* **28**, 235–248.

Schönholzer, F., Hahn, D., Zarda, B. & Zeyer, J. 2002 Automated image analysis and *in situ* hybridization as tools to study bacterial populations in food resources, gut and cast of *Lumbricus terrestris* L. *J. Microbiol. Methods* **48**, 53–68.

Servais, P., Billen, G. & Hascoët, M.-C. 1987 Determination of the biodegradable fraction of dissolved organic matter in water. *Wat. Res.* **21**, 445–450.

Siegrist, R. J. 1987 Soil clogging during subsurface wastewater infiltration as affected by effluent composition and loading rate. *J. Environ. Qual.* **16**, 181–187.

Soares, M. I. M., Belkin, S. & Abeliovich, A. 1989 Clogging of microbial denitrification sand columns: gas bubbles or biomass accumulation? *J. Wat. Wastewat. Res.* **22**, 20–24.

Taylor, S. W. & Jaffé, P. R. 1990 Biofilm growth and related changes in the physical properties of a porous media. 1. Experimental investigation. *Wat. Resour. Res.* **26**, 2153–2159.

Thullner, M., Zeyer, J. & Kinzelbach, W. 2002*a* Influence of microbial growth on hydraulic properties of pore networks. *Transp. Porous Media* **49**, 99–122.

Thullner, M., Mauclaire, L., Schroth, M. H., Kinzelbach, W. & Zeyer, J. 2002*b* Interaction between water flow and spatial distribution of microbial growth in a two-dimensional flow field in saturated porous media. *J. Contam. Hydrol.* **58**, 169–189.

Urfer, D., Huck, P. M., Booth, S. D. J. & Coffey, B. M. 1997 Biological filtration for BOM and particle removal: a critical review. *J. Am. Wat. Wks Assoc.* **89**, 83–98.

Vandevivere, P. & Baveye, P. 1992*a* Effect of bacterial extracellular polymers on the saturated hydraulic conductivity of sand columns. *Appl. Environ. Microbiol.* **58**, 1690–1698.

Vandevivere, P. & Baveye, P. 1992*b* Saturated hydraulic conductivity reduction caused by aerobic bacteria in sand columns. *Soil Sci. Soc. Am. J.* **56**, 1–13.

Vandevivere, P., Baveye, P., Sanchez de Lozada, D. & DeLeo, P. 1995 Microbial clogging of saturated soils and aquifer material: evaluation of mathematical models. *Wat. Resour. Res.* **31**, 2173–2180.

Weber-Shirk, M. L. & Dick, R. I. 1997*a* Physical-chemical mechanisms in slow sand filters. *J. Am. Water Works Assoc.* **89**, 87-100

Weber-Shirk, M. L. & Dick, R. I. 1997*b* Biological mechanisms in slow sand filters. *J. Am. Wat. Wks Assoc.* **89**, 73–83.

Wood, W. W. & Bassett, R. L. 1975 Water quality changes related to the development of anaerobic conditions during artificial recharge. *Wat. Resour. Res.* **11**, 553–558.

First received 13 January 2002; accepted in revised form 26 August 2003